

THE REACTION  $\gamma p \rightarrow p \rho^0$  WITH LINEARLY POLARIZED PHOTONS AT

2.8 and 4.7 GeV: CROSS SECTIONS AND THE  $\rho^0$  MASS SHIFT\*

H. H. Bingham, W. B. Fretter, K. C. Moffeit, W. J. Podolsky,  
M. S. Rabin, A. H. Rosenfeld, and R. Windmolders\*\*

Department of Physics and Lawrence Radiation Laboratory  
University of California, Berkeley, California 94720

J. Ballam, G. B. Chadwick, R. Gearhart, Z. G. T. Guiragossian,  
M. Menke, J. J. Murray, P. Seyboth, \*\*\* A. Shapira, †  
C. K. Sinclair, I. O. Skillicorn, ‡ and G. Wolff ††

Stanford Linear Accelerator Center  
Stanford University, Stanford, California 94305

R. H. Milburn

Tufts University, Medford, Massachusetts 02155

ABSTRACT

Rho photoproduction is studied at 2.8 and 4.7 GeV using a linearly polarized photon beam in a hydrogen bubble chamber. The dependence of the  $\rho^0$  mass shape on the momentum transfer is inconsistent with the Ross-Stodolsky factor. The production of  $\pi^+ \pi^-$  pairs in the s-channel c. m. helicity-conserving p-wave state accounts for almost all events in the  $\rho$  region. Evidence is presented for an interference of  $\rho^0$  production with background. The data are compared with the Söding model and total and differential cross sections for  $\rho^0$  production are presented.

(Submitted to Phys. Rev. Letters)

\* Work supported in part by the U. S. Atomic Energy Commission and the National Science Foundation.

\*\* Visitor from Laboratoire Interuniversitaire des Hautes Energies, Brussels, Belgium.

\*\*\* On leave from Max-Planck-Institut für Physik und Astrophysik, München, Germany.

† On leave from Weizmann Institute, Rehovoth, Israel.

‡ On leave from Brookhaven National Laboratory, Upton, New York.

†† On leave from DESY, Hamburg, Germany.

Previous studies of  $\rho^0$  photoproduction in the reaction



have shown that the rho shape is skewed with respect to a p-wave Breit-Wigner resulting in an apparent mass shift of the order of 40 MeV.<sup>1,2</sup> These observations have necessitated the use of models to fit the data, and because no model has been preferred experimentally, the  $\rho^0$  production cross section has been uncertain to  $\sim 20\%$ . We present model-independent cross sections for production of  $\pi^+ \pi^-$  pairs from reaction (1) in the s-channel c.m. helicity-conserving p-wave state which dominates in the  $\rho$  region.<sup>3</sup> We also determined the  $\rho^0$  production cross sections using the Söding model,<sup>4</sup> which was found to agree with the data.

The results published here are part of a detailed study of photoproduction with a bubble chamber using a linearly polarized photon beam. We obtained  $90 \pm 4$  events/ $\mu b$  and  $149 \pm 6$  events/ $\mu b$  at 2.8 and 4.7 GeV, respectively. Measurements of the total  $\gamma p$  cross section at 1.4, 2.8 and 4.7 GeV have already been reported;<sup>5a</sup> the analysis of the  $\rho^0$  decay distributions and results on  $\omega$  and  $\Delta^{++}$  production are given elsewhere.<sup>3</sup>

## I. EXPERIMENTAL SETUP

The 82-inch hydrogen bubble chamber at SLAC was exposed to a photon beam obtained by Compton backscattering a linearly polarized ruby laser beam on high energy electrons. By collimating both the electron and the backscattered photon beam to less than  $10^{-5}$  radians the width at half maximum of the photon energy spectrum is  $\pm 2.6\%$  and  $\pm 3.3\%$  at 2.8 and 4.7 GeV, respectively. The average degree of linear polarization as calculated for the Compton scattering process is 94% and 92%, respectively. Most of the film was taken with 70-80 photons/picture. More details of the beam can be found elsewhere.<sup>5b</sup>

## II. ANALYSIS OF THE FILM

Approximately 292,000 and 454,000 photographs were taken resulting in a total of 11,000 and 19,000 events at 2.8 and 4.7 GeV, respectively. All pictures were double scanned, and the combined scanning efficiency was found to be greater than 99% for all topologies. About 70% of the events were measured on conventional measuring machines and the remainder on the LRL Spiral Reader II. The events were analyzed using the programs TVGP and SQUAW. After three measurement passes less than 2% of the 3-prong events remained to be measured. The fraction of 3-prong events which could not be measured due to secondary scatters or track obscuration was 5%. The calculated effective-mass error for  $\pi\pi$  pairs of reaction (1) near the  $\rho$  mass was  $\pm 5$  MeV. There were 2854 and 2910 events at 2.8 and 4.7 GeV, respectively, which gave a 3C fit to reaction (1) consistent with the observed ionization and with a fitted photon energy in the interval  $2.4 < E_\gamma < 3.3$  GeV or  $4.1 < E_\gamma < 5.3$  GeV. The effects of possible contamination by wide-angle electron-positron pair production and scanning losses of events with a short proton recoil track were estimated.<sup>6</sup> The corrections were found to be negligible for events with  $|t| > 0.02$  GeV<sup>2</sup> ( $t$  is the square of the four-momentum transfer between incoming and outgoing proton) and consequently, for all further studies only events with  $|t| > 0.02$  GeV<sup>2</sup> were considered.

## III. RESULTS

The corrected total cross sections for reaction (1) are given in Table I and agree with other experiments.<sup>2</sup> Figure 1 shows the  $\pi^+\pi^-$  mass distributions for various  $t$  intervals. The dominant feature is  $\rho^0$  production;  $\Delta^{++}(1236)$  production, which is also present in reaction (1), is discussed elsewhere.<sup>3</sup> We have looked

in the  $\pi^+\pi^-$  mass distributions for the production of higher mass mesons, in particular the vector mesons  $\rho'$  and  $\rho''$  with masses of  $\sim 1.3$  and  $\sim 1.7$  GeV predicted by the Veneziano model.<sup>7</sup> The upper limits (1 s. d.) on their production cross sections at 4.7 GeV are  $0.5 \mu\text{b}$  and  $0.4 \mu\text{b}$ , respectively, assuming for both  $\rho'$  and  $\rho''$  a width of 200 MeV and decay into  $\pi^+\pi^-$  only. These upper limits agree with other experiments<sup>8</sup> but are still consistent with a recent Veneziano model calculation.<sup>9</sup>

In order to test the Ross-Stodolsky factor<sup>10</sup> we have multiplied the p-wave Breit-Wigner for the  $\rho$  by a factor of  $(M_\rho/M_{\pi\pi})^{n(t)}$ . Maximum likelihood fits have been made to the events of reaction (1) allowing for  $\rho^0$  and  $\Delta^{++}(1236)$  production and a phase space term<sup>11</sup> and fitting these contributions together with the parameter  $n(t)$  as a function of  $t$ . The fits describe the  $\pi^+\pi^-$  mass spectra well, as shown by the dashed curves in Fig. 1. The fitted values for  $n(t)$  are shown in Fig. 2c, d. In contrast to the prediction of Ross and Stodolsky, namely  $n(t=0) = 4$ , the parameter  $n$  is  $\sim 5$  near  $t=0$ ; it drops to zero around  $|t|=0.5$  GeV<sup>2</sup>.

The analysis of the  $\rho^0$  decay in this experiment has shown<sup>3</sup> that for  $|t| < 0.4$  GeV<sup>2</sup> the  $\rho^0$  decay angular distribution is

$$W(\theta, \psi) = \frac{3}{8\pi} \left\{ \sin^2 \theta + P_\gamma \sin^2 \theta \cos 2\psi \right\} \quad (2)$$

Here  $\theta$  is the polar angle of the decay  $\pi^+$ ,  $\psi$  is the polarization angle defined as  $\psi = \phi - \Phi$ , where  $\phi$  is the azimuthal angle of the  $\pi^+$  with respect to the production plane,  $\Phi$  is the angle between the photon electric vector and the production plane, and  $P_\gamma$  is the degree of linear polarization of the photon. All angles are calculated in the  $\pi^+\pi^-$  helicity system. Equation (2) can be expressed in terms of the moments  $Y_0^0(\theta, \psi)$ ,  $Y_2^0(\theta, \psi)$  and  $\text{Re } Y_2^2(\theta, \psi)$ . Because of its  $\psi$  dependence,  $\text{Re } Y_2^2(\theta, \psi)$  is the least affected by background and therefore has been used to determine the intensity of the s-channel c. m. helicity-conserving p-wave  $\pi\pi$

contribution,  $\Pi$ :

$$\Pi = \frac{1}{P_\gamma} \sqrt{\frac{40\pi}{3}} \sum \text{Re } Y_2^2 \quad (3)$$

where the summation is over all events. The dots marked on the histograms of Fig. 1 show  $\Pi$  as a function of  $M_{\pi\pi}$  for different  $t$  intervals. We notice that a) in the  $\rho$  region  $\Pi$  accounts for almost all events and shows the same skewing as the mass distributions; b) above  $M_{\pi\pi} = 1 \text{ GeV}$   $\Pi$  is zero within errors, again emphasizing the absence of higher vector mesons; this also shows that the background which is present above 1 GeV does not contribute to  $\text{Re } Y_2^2$ . The total helicity-conserving p-wave cross section (corrected for the interval  $|t| < 0.02 \text{ GeV}^2$ ) is given in Table I.

Further analysis of the  $\pi\pi$  angular distribution was made by studying the  $M_{\pi\pi}$  dependence of other  $Y_L^M(\theta, \psi)$  moments. In Fig. 3 we show the moments  $Y_2^0$  and  $Y_4^0$  at 4.7 GeV. The  $Y_2^0$  moment shows the behavior expected for the  $\sin^2 \theta$  decay of the  $\rho^0$ . The positive values of  $Y_2^0$  above 1 GeV are due to the  $\Delta^{++}$  reflection. The moment  $Y_4^0$  shows a distinctive interference pattern in the  $\rho$  region which can be interpreted as an interference between the  $\rho^0$  and a  $\pi^+\pi^-$  state of spin  $J \geq 3$ .<sup>12</sup>

In view of the observed interference effect we compared our data with the model of Söding,<sup>4, 13</sup> which explains the  $\rho$  mass shift in terms of an interference between the  $\rho^0$  production and a Drell-type background amplitude.<sup>14</sup> The solid lines shown in Figs. 1-3 were calculated from the Söding model after fitting the ratio of the total  $\rho^0$  and Drell cross sections,  $\sigma_\rho/\sigma_D$ , and allowing for  $\Delta^{++}$  production and an additional background term. The fitted values of  $\sigma_\rho/\sigma_D$  are shown in Figs. 2e, f as a function of  $t$ . The Söding model describes the  $t$  dependence of the  $\pi^+\pi^-$  mass distributions and of  $\sigma_\rho/\sigma_D$ , and consequently, the related dependence

of the exponential slope of the  $t$  distribution on the  $\pi^+\pi^-$  mass<sup>2,15</sup> (see Fig. 2a, b). The shape of the interference pattern observed for  $Y_4^0$  is also correctly predicted (see Fig. 3). The total  $\rho^0$  production cross sections obtained by fitting the Söding model to our data (and correcting for the interval  $|t| < 0.02 \text{ GeV}^2$ ) are given in Table I.

In Fig. 4 and Table II we give the differential cross sections obtained from fits with the Söding model, those for  $\bar{\nu}\nu$  and also those resulting from the parametrization  $(M_\rho/M_{\pi\pi})^{n(t)}$ . Fitting the differential cross section values for  $|t| < 0.4 \text{ GeV}^2$  to the form  $d\sigma/dt = d\sigma/dt(t=0) \exp(At)$  we obtain  $d\sigma/dt(t=0)$  and  $A$  as given in Table I. We remark that for  $|t| < 0.4 \text{ GeV}^2$  the differential cross sections and the slopes obtained for  $\bar{\nu}\nu(t)$  and for the  $\rho^0$  cross sections fitted with the parametrization  $(M_\rho/M_{\pi\pi})^{n(t)}$  or with the Ross-Stodolsky factor agree within errors. The  $\rho^0$  cross sections obtained from fitting the Söding model lead to smaller values for the forward differential cross section (by  $\sim 25\%$ ) and for the slope.

The forward  $\rho^0$  cross sections obtained from fitting the Söding model are about  $60 \mu\text{b}/\text{GeV}^2$  smaller at both energies than the values quoted by the DESY-MIT group,<sup>16</sup> who also used an interference model.

#### IV. CONCLUSIONS

We have observed a variation of the  $\rho$  mass shape as a function of  $t$ , a variation of the exponential slope of the  $t$  distribution with  $M_{\pi\pi}$  and an interference of the  $\rho^0$  amplitude with background. These features are inconsistent with a model using only the Ross-Stodolsky factor to explain the  $\rho^0$  mass shift, but are well described by the interference model of Söding. The production of  $\pi^+\pi^-$  pairs in the s-channel c.m. helicity-conserving p-wave state, determined in a model-independent way, accounts for almost all events in the  $\rho$  region and shows the same skewing as the  $\pi^+\pi^-$  mass distributions.

#### ACKNOWLEDGEMENTS

Our thanks go to the SLAC accelerator operation group, and to R. Watt and the 82-inch bubble chamber crew. We are also indebted to the scanners at SLAC and Berkeley and in particular to W. Hendricks, Mrs. Tartar and A. Wang for their coordinating effort. The help of W. Graves is gratefully acknowledged.

#### REFERENCES AND FOOTNOTES

1. H. R. Crouch et al., Proceedings of the International Symposium on Electron and Photon Interactions at High Energies, 1965, edited by G. Höhler et al., (Deutsche Physikalische Gesellschaft, Hanau, Germany, 1966) Vol. II, p. 13.
2. Aachen-Berlin-Bonn-Hamburg-Heidelberg-München Collaboration, Phys. Rev. 175, 1669 (1968), and references given therein.
3. SLAC-Berkeley-Tufts Collaboration, Report Nos. SLAC-PUB-728, SLAC-PUB-729, SLAC-PUB-730, Stanford Linear Accelerator Center, (1970) to be published.
4. P. Söding, Phys. Letters 19, 702 (1965); see also A. S. Krass, Phys. Rev. 159, 1496 (1967).
- 5a. SLAC-Berkeley-Tufts Collaboration, Phys. Rev. Letters 23, 498 (1969); ibid. 23, 817 (1969).
- b. J. J. Murray and P. Klein, "A backscattered laser beam for the 82" bubble chamber," Report No. SLAC-TN-67-19; C. K. Sinclair, J. J. Murray, P. Klein, and M. Rabin, IEEE Trans. on Nucl. Sci. 16, 1065 (1969).
6. We scanned both for 3-prong and 2-prong events, the latter originating mainly from the reaction  $yp \rightarrow p\pi^+\pi^-$  (in which the proton momentum was too small to give a visible track) and from wide-angle pair production (WAP).

The number of WAP events which could have been confused with events of reaction (2) has been calculated using the Bethe-Heitler cross section formula.

(W. Heitler, The Quantum Theory of Radiation, (Oxford University Press, London, 1954, 3rd edition); p. 257.) About 2% of the events of reaction (2) were found to be WAP candidates. After removing the WAP candidates the  $t$  distribution was examined for scanning losses as a function of  $M_{\pi\pi}$ . Assuming that the  $t$  distribution is of the form  $\exp(At)$  and allowing  $A$  to vary with  $M_{\pi\pi}$  the scanning losses for  $|t| < 0.02 \text{ GeV}^2$  were found to be 1% at 2.8 GeV and 5% at 4.7 GeV. Both WAP contamination and scanning losses were found to be negligible for  $|t| > 0.02 \text{ GeV}^2$ .

7. J. A. Shapiro, Phys. Rev. 179, 1345 (1969).
8. A. Silverman, Proceedings of the 4th Internat'l. Symposium on Electron and Photon Interactions at High Energies, Liverpool, 1969, ed. by D. W. Braben, p. 71.
9. H. Satz and K. Schilling, CERN Preprint TH-1127, January 1970. These authors explain the  $\rho$  mass shift, but in contradiction to experiment their model predicts  $t$ -channel helicity conservation for  $\rho^0$  production.
10. M. Ross and L. Stodolsky, Phys. Rev. 149, 1172 (1966).
11. For the density distribution on the Dalitz plot we use formula (A1) of Ref. 2 with the addition of the factors  $\exp(7t)$  and  $\exp(7.1t_\Delta)$  ( $t_\Delta$  = square of four-momentum transfer between incoming proton and outgoing  $\Delta^{++}$ ) which multiply the  $\rho$  and  $\Delta^{++}$  Breit-Wigner terms.
12. At 2.8 GeV the moment  $Y_4^0$  does not show a statistically significant interference effect. This is probably due to the large  $\Delta^{++}$  production, which plays only a minor role at 4.7 GeV.

13. The predictions of the Söding model have been calculated using a Monte-Carlo program written by P. Söding. The formulae employed differ from those given in Ref. 4 in the following points: the pion nucleon scattering is calculated from the phase shift data keeping only the spin nonflip term; the rho amplitude is assumed to be helicity conserving in the s-channel c. m. s. The  $\rho$  mass,  $M_\rho$ , and width,  $\Gamma_\rho$ , used in the determination of the differential cross sections were obtained from fits to the events in the interval  $0.02 < |t| < 0.5 \text{ GeV}^2$ . The resulting values were  $M_\rho = 765 \pm 3 \text{ MeV}$  ( $760 \pm 3 \text{ MeV}$ ) and  $\Gamma_\rho = 132 \pm 6 \text{ MeV}$  ( $141 \pm 5 \text{ MeV}$ ) at  $2.8 \text{ GeV}$  ( $4.7 \text{ GeV}$ ). We note that there are theoretical difficulties with the Söding model, namely gauge invariance, neglect of a possible real part of the  $\rho^0$  production amplitude, possible double counting effects and the omission of other diagrams as remarked upon by D. R. Yennie (private communication).
14. The  $\rho$  mass shift has also been discussed by G. Kramer and J. L. Uretsky, Phys. Rev. 181, 1918 (1969), and P. D. Mannheim and U. Maor, UC-Berkeley preprint (1970), to be published.
15. M. Davier et al., Report No. SLAC-PUB-613, Stanford Linear Accelerator Center, and Phys. Rev., to be published.
16. H. Alvensleben et al., Phys. Rev. Letters 23, 1058 (1969).

TABLE I

Total cross sections for  $\gamma p \rightarrow p\pi^+\pi^-$ ; total and forward differential cross sections and slope A for production of  $\pi^+\pi^-$  pairs in the s-channel c.m. helicity conserving p-wave state ( $II$ ) and for  $\rho^0$  production as determined from fits with the Söding model.

$E_\gamma$ (GeV)	$\sigma(\gamma p \rightarrow p\pi^+\pi^-)$ ( $\mu$ b)	hel. cons. p-wave ( $II$ )		$\rho^0$ production		
		$\sigma$ ( $\mu$ b)	$\frac{d\sigma}{dt}(t=0)$ ( $\mu$ b/GeV $^2$ )	A (GeV $^{-2}$ )	$\sigma$ ( $\mu$ b)	$\frac{d\sigma}{dt}(t=0)$ ( $\mu$ b/GeV $^2$ )
2.8	$31.4 \pm 1.3$	$18.9 \pm 1.1$	$144 \pm 13$	$7.5 \pm 0.6$	$16.4 \pm 1.0$	$93 \pm 7$
4.7	$20.2 \pm 0.8$	$13.5 \pm 1.0$	$102 \pm 8$	$7.2 \pm 0.5$	$14.4 \pm 0.7$	$80 \pm 5$

TABLE II

Differential cross sections  $d\sigma/dt(\mu\text{b}/\text{GeV}^2)$  for production of  $\pi^+\pi^-$  pairs in the s-channel c. m. helicity conserving p-wave state( $\Pi$ ) and for  $\rho^0$  production\* at 2.8 and 4.7 GeV

$-t(\text{GeV}^2)$	$E_\gamma = 2.8 \text{ GeV}$		$E_\gamma = 4.7 \text{ GeV}$	
	$\Pi$	$\rho^0$	$\Pi$	$\rho^0$
0.02 - 0.05	119 $\pm$ 11	78 $\pm$ 6	74 $\pm$ 7	65 $\pm$ 4
0.05 - 0.075	89 $\pm$ 10	64 $\pm$ 6	64 $\pm$ 7	56 $\pm$ 5
0.075 - 0.10	67 $\pm$ 10	58 $\pm$ 6	52 $\pm$ 6	49 $\pm$ 4
0.10 - 0.15	56 $\pm$ 6	46 $\pm$ 4	45 $\pm$ 4	41 $\pm$ 3
0.15 - 0.20	37 $\pm$ 5	39 $\pm$ 4	37 $\pm$ 4	33 $\pm$ 2
0.20 - 0.25	29 $\pm$ 4	25 $\pm$ 4	16 $\pm$ 3	20 $\pm$ 2
0.25 - 0.30	19 $\pm$ 4	22 $\pm$ 2	13 $\pm$ 3	20 $\pm$ 1.4
0.30 - 0.35	15 $\pm$ 4	15 $\pm$ 4	9.1 $\pm$ 2.2	12.4 $\pm$ 1.6
0.35 - 0.40	7.6 $\pm$ 3.0	11.4 $\pm$ 2.4	6.8 $\pm$ 1.8	9.0 $\pm$ 1.5
0.40 - 0.50	4.4 $\pm$ 1.5	6.2 $\pm$ 1.1	5.6 $\pm$ 1.1	6.2 $\pm$ 1.0
0.50 - 0.70	3.2 $\pm$ 0.8	2.4 $\pm$ 0.6	0.6 $\pm$ 0.5	2.4 $\pm$ 0.4
0.7 - 1.0	1.0 $\pm$ 0.6	2.2 $\pm$ 0.4	0.9 $\pm$ 0.3	0.78 $\pm$ 0.16
1.0 - 1.5	0.6 $\pm$ 0.4	0.76 $\pm$ 0.22	0.15 $\pm$ 0.20	0.34 $\pm$ 0.08
1.5 - 2.5	0. $\pm$ 0.17	0.17 $\pm$ 0.09	0.20 $\pm$ 0.09	0.067 $\pm$ 0.027
2.5 - $ t _{\text{max}}$	0. $\pm$ 0.11	0.23 $\pm$ 0.08	0.015 $\pm$ 0.013	0.016 $\pm$ 0.008

\* The differential cross sections for  $\rho^0$  production for  $|t| < 0.7 \text{ GeV}^2$  were determined using the Söding model, for  $|t| > 0.7 \text{ GeV}^2$  describing  $\rho^0$  production by a p-wave Breit-Wigner.

### FIGURE CAPTIONS

1.  $\pi^+\pi^-$  mass distributions for events of the reaction  $\gamma p \rightarrow p\pi^+\pi^-$ . The helicity-conserving p-wave intensity  $\Pi$  (see text) is shown by the points  $\dagger$ . The curves give the results of a maximum likelihood fit using for the  $\rho^0$  the parametrization  $(M_\rho/M_{\pi\pi})^{n(t)}$  (---) and the Söding model (—).
2. Reaction  $\gamma p \rightarrow p\pi^+\pi^-$ : (a),(b) The exponential slope of the  $t$  distribution as a function of the  $\pi^+\pi^-$  mass taking all events in a given  $\pi^+\pi^-$  mass bin and with  $0.02 < |t| < .4 \text{ GeV}^2$ . The curves show the result of the Söding model. (c),(d) Fitted values for  $n(t)$  using the parametrization  $(M_\rho/M_{\pi\pi})^{n(t)}$ . (e),(f) Ratio of the fitted  $\rho^0$  production to Drell cross sections,  $\sigma_\rho(t)/\sigma_D(t)$ . The curves show the predictions of the Söding model.
3. Reaction  $\gamma p \rightarrow p\pi^+\pi^-$ : the moments  $Y_2^0(\theta, \psi)$  and  $Y_4^0(\theta, \psi)$  in the helicity frame as a function of  $M_{\pi\pi}$  for  $0.02 < |t| < 0.4 \text{ GeV}^2$ . The curves show the results of the Söding model.
4. Reaction  $\gamma p \rightarrow p\pi^+\pi^-$ : Differential cross sections as a function of  $t$  for the helicity-conserving p-wave contribution  $\Pi(\dagger)$ , for  $\rho^0$  production as obtained from fits with the Söding model ( $\dagger$ ) and using the parametrization  $(M_\rho/M_{\pi\pi})^{n(t)}(\dagger)$ .

$$\gamma p \rightarrow p \pi^+ \pi^-$$

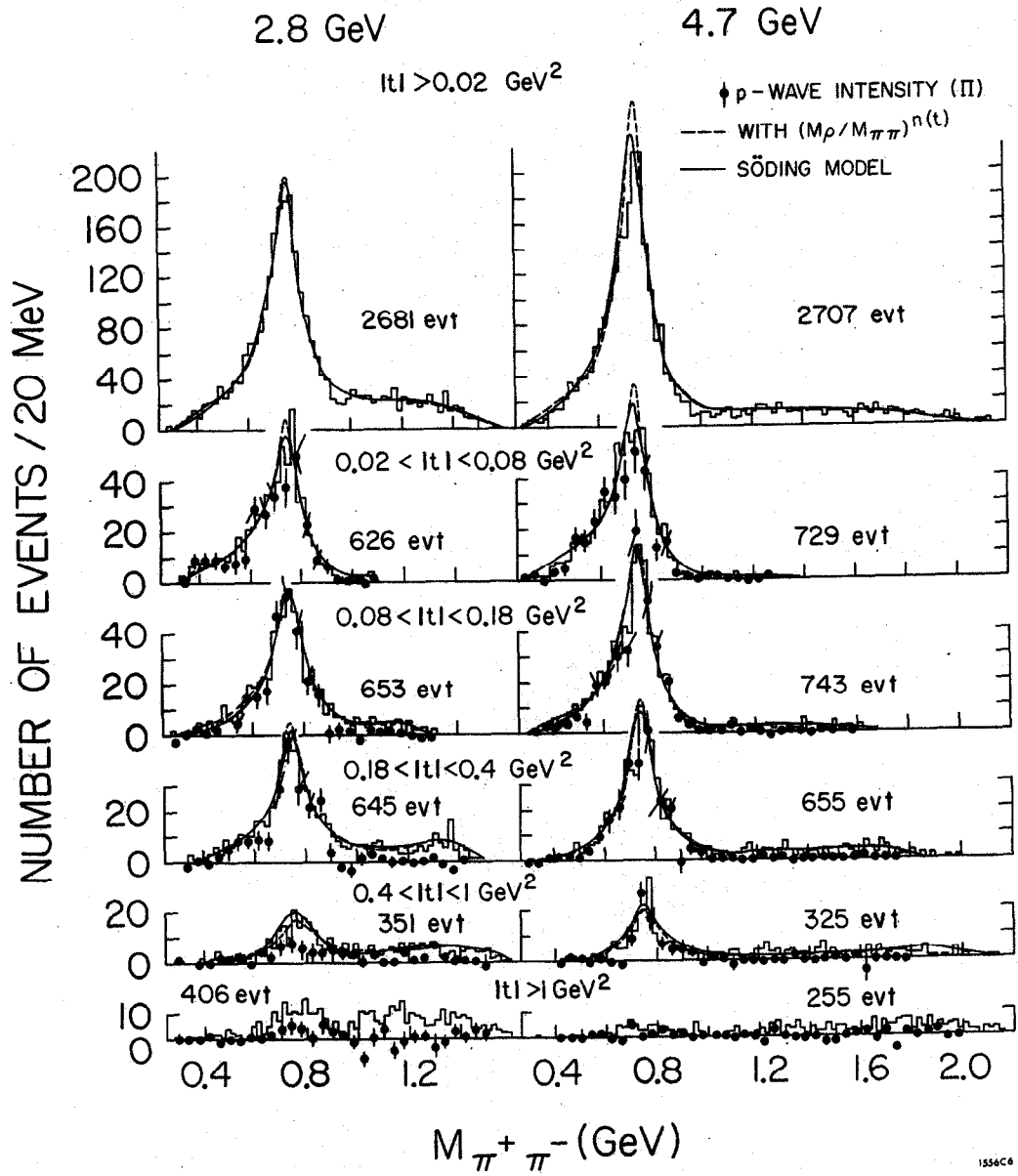
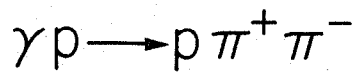


Fig. 1



2.8 GeV

4.7 GeV

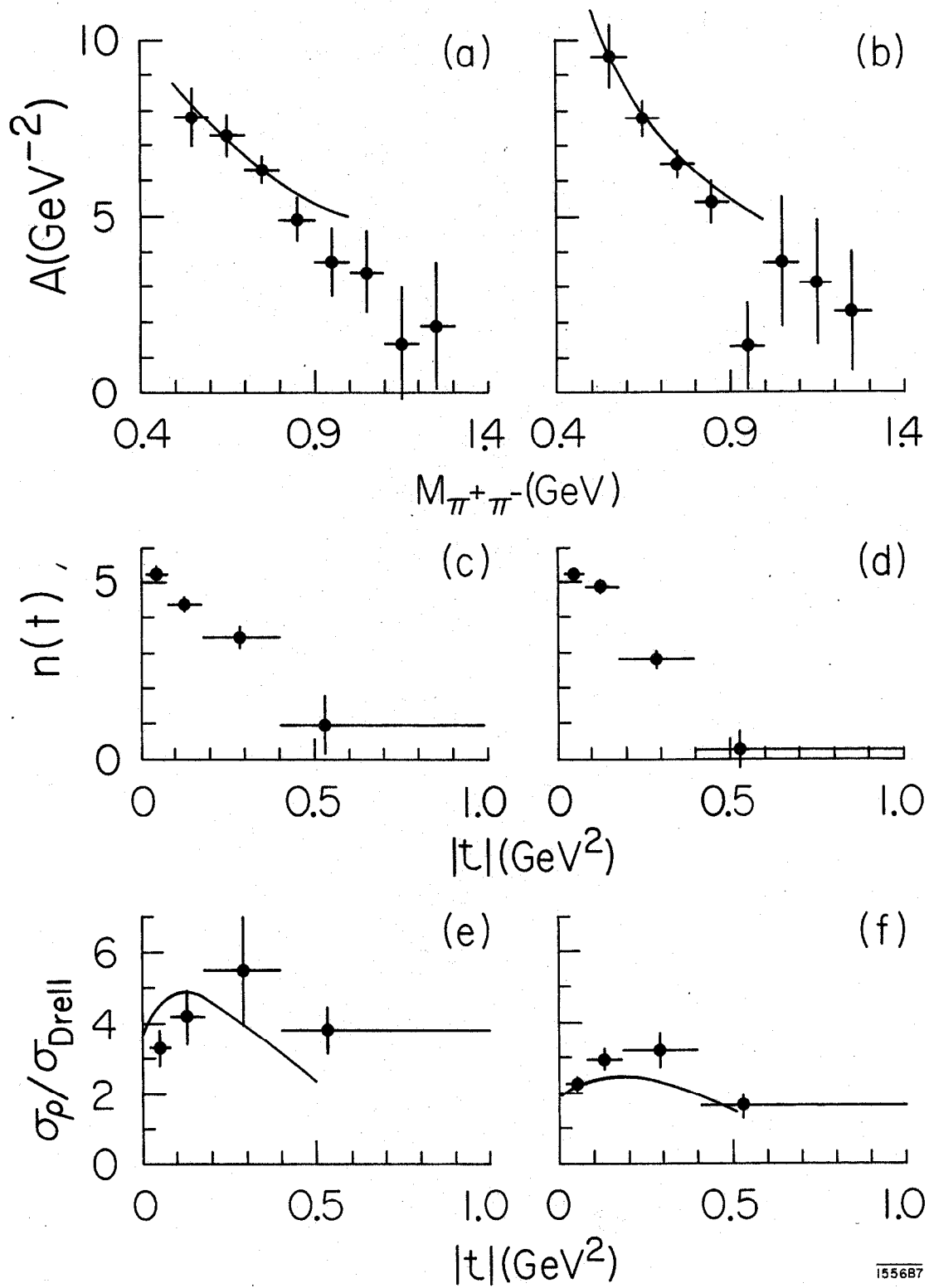
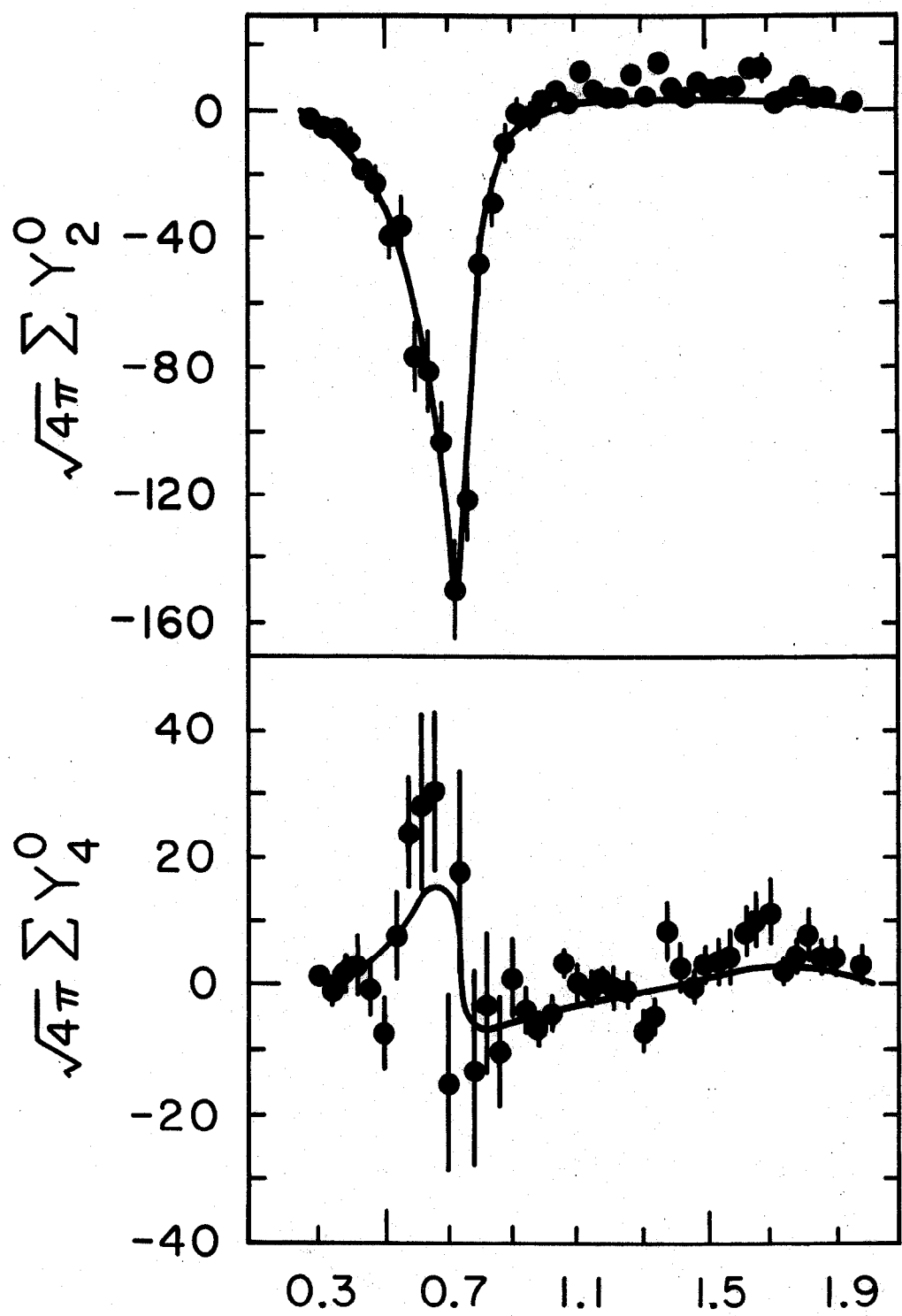


Fig. 2

4.7 GeV  $\gamma p \rightarrow p\pi^+\pi^-$



$M_{\pi^+\pi^-}$  (GeV)

1556A1

Fig. 3

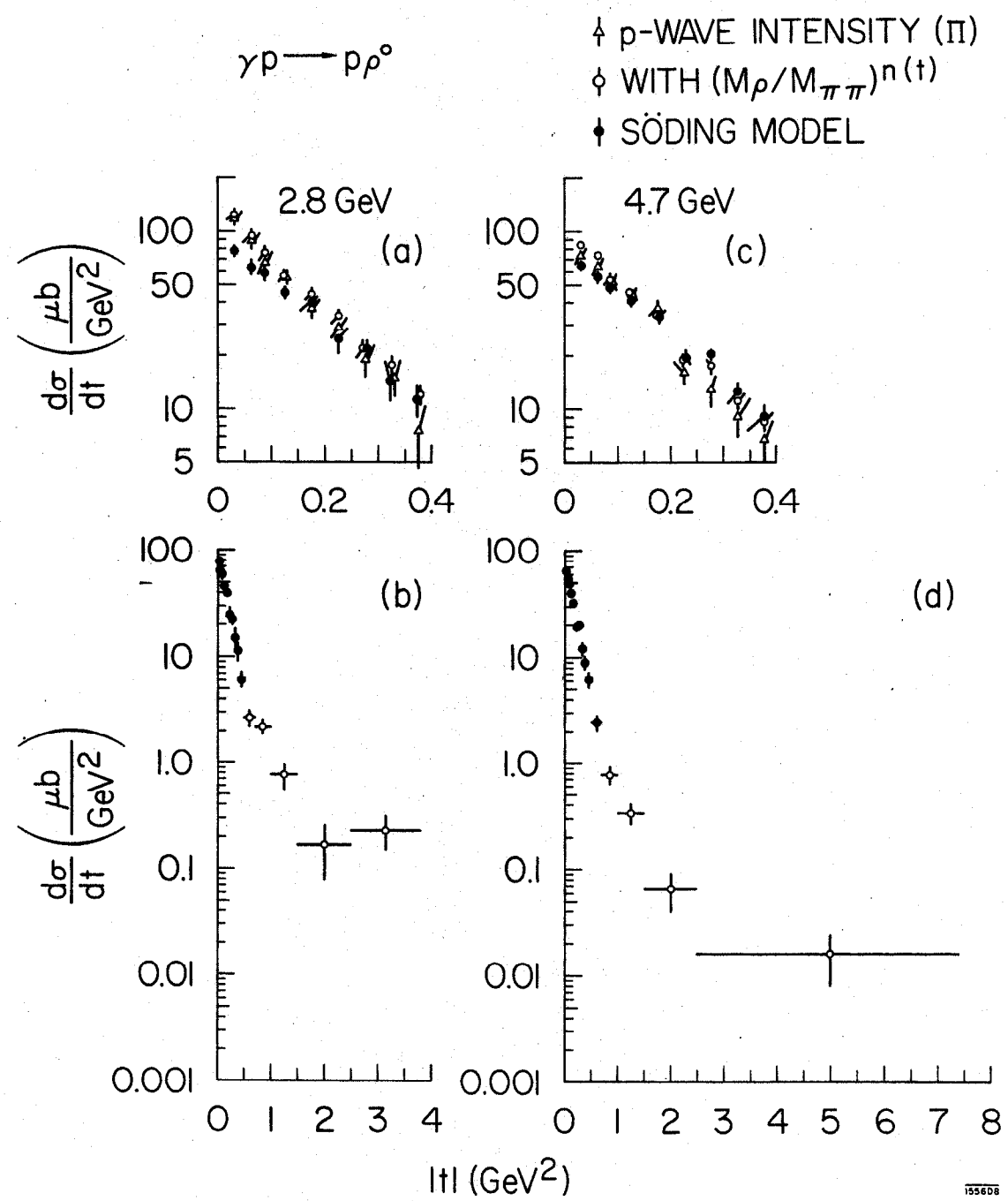


Fig. 4